JOURNAL OF VIROLOGY, Jan. 1992, p. 420–431
0022-538X/92/010420-12$02.00/0

Vol. 66, No. 1

In Vivo Resolution of Circular Plasmids Containing Concatemer Junction Fragments from Minute Virus of Mice DNA and Their Subsequent Replication as Linear Molecules

SUSAN F. COTMORE[1] AND PETER TATTERSALL[1,2]*

Departments of Laboratory Medicine[1] and Genetics,[2] Yale University School of Medicine, 333 Cedar Street, New Haven, Connecticut 06510

Received 6 August 1991/Accepted 26 September 1991

During replication of their linear, single-stranded DNA genomes, parvoviruses generate a series of concatemeric duplex intermediates. We have cloned, into *Escherichia coli* plasmids, junction fragments from these palindromic concatemers of minute virus of mice DNA spanning both the right end-to-right end (viral 5′ to 5′) and left end-to-left end (viral 3′ to 3′) fusions. When mouse cells were transfected with these circular plasmids and superinfected with minute virus of mice, the viral junctions were resolved and the plasmids replicated as linear chromosomes with vector DNA in their centers and viral DNA at their termini. Resolution did not occur when the concatemer joint was replaced by a different palindromic sequence or when the transfected cells were not superinfected, indicating the presence of latent origins of replication which could only be activated by a viral *trans*-acting factor(s). Moreover, the products of resolution and replication from the two termini were characteristically different. Analysis of individual terminal fragments showed that viral 5′ (right-end) sequences were resolved predominantly into "extended" structures with covalently associated copies of the virally encoded NS-1 polypeptide, while bridges derived from the 3′ (left) end resolved into both NS-1-associated extended termini and lower-molecular-weight "turn-around" forms in which the two DNA strands were covalently continuous. This pattern of resolution exactly coincides with that seen at the two termini of replicative-form intermediates in normal virus infections. These results demonstrate that the bridge structures are authentic substrates for resolution and indicate that the frequency with which extended versus turn-around forms of each terminus are generated is an intrinsic property of the telomere.

All parvoviruses have linear nonpermuted DNA genomes of about 5 kb in which a long, single-stranded coding region is bracketed by short terminal palindromic sequences capable of folding into hairpin duplexes (38). Analysis of defective interfering particles (21) and studies with recombinant viruses in which selectable marker genes were incorporated into a truncated viral genome (36) suggest that all the *cis*-acting information necessary for viral DNA replication and encapsidation resides within about 200 nucleotides of each telomere. It was originally thought that these viruses might replicate their genomes by a simple mechanism, dubbed rolling-hairpin synthesis, in which self-priming at the 3′ terminus was coupled with a hairpin transfer step during which the palindromic sequence at the 5′ end of one strand was copied onto the 3′ end of its complement (5, 43). Such a mechanism is compatible with the observed replication products of parvoviruses, such as the adeno-associated viruses (AAV), which have inverted terminal repeats and can be partially reproduced in vitro with hairpinned AAV termini and infected-cell extracts (40) or purified, virally encoded proteins (25). However, this mechanism is difficult to reconcile with the observed replication products of viruses which have unique termini (1, 2, 8, 18). Parvoviral palindromes contain a number of mispaired bases, and replication by a simple hairpin transfer mechanism must result in the generation of two complementary forms of each palindrome designated "flip" and "flop." Both of these forms are found at each end of the AAV genome and at the right (5′) end of viruses with unique termini. However, in the latter viruses, only a single sequence orientation (1, 2, 18) or a preponderance of one orientation (8) is observed at the left (3′) end.

To explain this discrepancy, Chen and colleagues proposed a kinetic hairpin transfer model (9, 47) in which disparities in the relative concentrations of the two forms are explained simply by differences in the rate constants for the nicking and repair/extension of each of the different orientations of the terminal palindromes of monomer replicative forms (RF) (9, 47). This model is mechanistically very different from the earlier modified rolling-hairpin model proposed by Astell and colleagues (1); this model explains the distribution of terminal forms observed in minute virus of mice (MVM) by invoking the asymmetric cleavage and duplication of multimeric linear replicative intermediates. During replication of their single-stranded genomes, parvoviruses generate both dimeric and tetrameric duplex concatemers (42, 48), which are palindromic arrangements of unit-length duplex molecules arranged in left end-to-left end (viral 3′-to-3′) and right end-to-right end (viral 5′-to-5′) orientations, respectively (48). To accommodate a self-priming mechanism with the generation of all left-end termini in a unique sequence orientation, Astell and colleagues (1) suggested that this end of the genome might be excised from the duplex bridge region of dimeric DNA by an enzyme analogous to the nicking-joining enzyme encoded by gene A of bacteriophage ϕX174. Consequently, this model predicts that concatemeric forms of the MVM genome, specifically 3′-to-3′ dimers, are obligatory replicative intermediates in the process of viral DNA replication. In contrast, the kinetic hairpin transfer model does not ascribe any particular role to the multimeric forms of viral RF DNA produced during

* Corresponding author.

infection and assumes that, once produced by replication, such molecules are resolved by simple staggered nicks followed by repair synthesis to produce monomers of opposite orientation at each end.

In light of these proposed models, we suggest that isolated bridge region fragments spanning the joints between such multimeric genomes might provide ideal substrates for analyzing concatamer resolution and that an understanding of this process would, in turn, indicate which of the apparently contradictory models most closely approximates the actual mechanism of parvoviral genome replication. In this report, we describe the cloning of MVM concatemer bridge region fragments spanning both the viral 3′-to-3′ and 5′-to-5′ junctions into *Escherichia coli* plasmids. We demonstrate the in vivo cleavage of these cloned junctions and the replication of the associated plasmid DNA as linear pseudoviral chromosomes following transfection into murine cells superinfected with MVM. In addition to showing that both of these junction regions are authentic substrates for resolution, we found that the products of resolution from the 3′-to-3′ bridge do indeed indicate that this process proceeds by a nicking-joining cleavage mechanism such as that proposed by Astell et al. (1).

MATERIALS AND METHODS

Cells and viruses. The prototype strain of MVM was grown in the mouse L-cell derivative A9 ouab^{r}11 or subclone iD5 of hybrid somatic cell line Hyb1/11, which was formed by fusion of A9 ouab^{r}11 cells with the murine T-cell lymphoma EL4. Cells were maintained in asynchronous cultures as previously described (43).

Molecular cloning of concatemer junction fragments. (i) Derivation of pLEB-2049, pLEB-711, and pREB-1412. Viral progeny and RF DNAs were obtained from 2×10^8 A9 cells 28 h after infection with the prototype strain of MVM [MVM(p)] at a multiplicity of infection (MOI) of 30 PFU per cell by a modified Hirt procedure (24). The DNA was digested with the following restriction enzymes: (i) *Eco*RI, cutting at nucleotide 1084 to yield a left-end bridge fragment of 2,049 bp (to give clone pLEB-2049); (ii) *Pst*I, cutting at nucleotide 415 to give a left-end bridge of 711 bp (to give clone pLEB-711); and (iii) *Xba*I, cutting at nucleotide 4342 to give a right-end bridge fragment of 1,412 bp (to give clone pREB-1412).

The digests were resolved on agarose gels, and DNA of the predicted sizes was purified by adsorption to glass beads after the agarose was dissolved in sodium iodide (Geneclean; Bio 101 Inc., La Jolla, Calif.). For the left-end bridge fragments, ethidium-visible bands of DNA were obtained, while for the right-end bridge fragments, we relied upon excision of the agarose from the correct region of the gel. Fragments were ligated into phosphatase-digested pUC18 vectors cut with *Eco*RI or *Pst*I or a pUC19 vector linearized at *Xba*I, as appropriate, and the products were transformed into the recombination-defective and restriction-negative *E. coli* SURE (Stratagene, La Jolla, Calif.), which carries *uvrC*, *umuC*, *sbcC*, *recB*, and *recJ* mutations and deletions of the *hsdR*, *mcrA*, *mcrB*, and *mrr* genes, or into the *recBC sbcB recF* strain JC8111 (6).

(ii) Subcloning of the left-end bridge, pLEB-157, and pIP-304. One of the 711-bp left-end *Pst*I bridge clone inserts was subsequently digested with *Dra*I, which cuts four times in the MVM sequence at nucleotides 136 and 170 on either side of the bridge. The 157-base bridge fragment was recloned into the *Sma*I site of pUC19 to give the construct pLEB-157. This *Pst*I bridge clone insert was also digested with *Nco*I, which cuts the viral DNA twice on either side of the bridge at MVM nucleotide 259 in the genomic sequence, and the cloned DNA was religated to give a clone containing two copies of the MVM sequence between nucleotides 260 and 415 arranged as a perfect 304-base palindrome. This clone was termed pIP-304 (IP denotes internal palindrome) and was only stable in JC8111.

Although transformation efficiencies were higher with SURE, the palindromic inserts showed a greater tendency for deletions in this bacterium, so JC8111 was used whenever such problems were encountered. Whenever tested, retransformation of recombinant plasmids into JM109 resulted in total deletion of the palindromes, with none of the intermediate deletion products normally encountered when infectious clones of MVM are replicated in such a bacterium (6).

Transfection and superinfection. Monolayers of A9 or iD5 cells were plated at 5×10^5 cells per 60-mm dish and transfected the next day with 5 μg of plasmid DNA in the presence of 20 μg of denatured salmon sperm DNA by coprecipitation with calcium phosphate (49) or with 5 μg of plasmid DNA in the absence of a carrier by delivery with lipofectin (Bethesda Research Laboratories, Gaithersburg, Md.) at 20 μg/ml in Opti-MEM medium (GIBCO, Grand Island, N.Y.) as described by Felgner and Holm (22). Sixteen to 20 h later, the cells were washed with medium containing 5% fetal calf serum and superinfected with MVM(p) at an MOI of 30 PFU per cell. Cells and medium were harvested 30 h after superinfection. Cells were scraped into the culture medium and separated by centrifugation. Cell pellets were resuspended in 400 μl of 0.02 M Tris-HCl–0.15 M NaCl–0.01 M EDTA (pH 7.5), flash-frozen on dry ice, and stored at −20°C.

Extractions, enzyme digestions, and immunoprecipitations. Aliquots of the cell suspension were digested with proteinase K at 200 μg/ml in the presence of 0.5% sodium dodecyl sulfate (SDS) at 60°C for 4 h, extracted with phenol and ether, and ethanol precipitated. Following RNase digestion (50 μg/ml for 1 h at 37°C), reextraction with phenol and ether, and ethanol precipitation, aliquots (generally derived from approximately 2.5×10^4 cells) were digested with restriction enzymes as described by the supplier (New England Biolabs, Beverly, Mass.).

For immunoprecipitations, samples of the original cell suspension were extracted with 2% SDS in the presence of 20 mm EDTA at 60°C for 20 min and immunoprecipitated with Formalin-fixed *Staphylococcus aureus* (Boehringer, Mannheim, Germany) as previously described (14), using a rabbit antiserum directed against a gel-purified bacterial fusion protein expressing the 84-amino-acid amino-terminal peptide of NS-1 (12). Precipitates were resuspended and digested at 37°C for 30 min with restriction enzymes in buffers provided by the enzyme supplier. Some samples were recentrifuged to separate NS-1-associated DNA fragments, which were still attached to the bacterial immunoadsorbent, from released DNA fragments in the supernatant. All samples were digested with proteinase K at 100 μg/ml in the presence of 0.5% SDS at 37°C for 30 min prior to electrophoresis.

Gel electrophoresis, Southern transfers, and probe synthesis. DNA was electrophoresed on neutral or alkaline agarose gels (28) and transferred to Hybond-N membranes (Amersham, Arlington Heights, Ill.) as described by the manufacturer. ^{32}P-labeled DNA probes were prepared with random DNA primers and the Klenow fragment of *E. coli* DNA

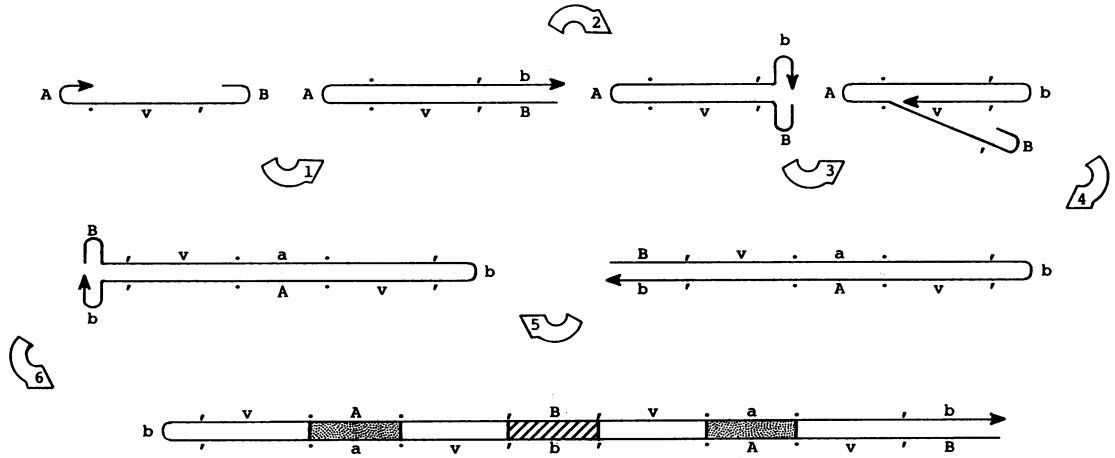

FIG. 1. The MVM genome is represented by a series of sequence blocks denoted by letters. Each uppercase and lower case letter denotes sequences complementary to each other. The 3′ palindrome is shown to the left of the parental genome in the upper left-hand corner and is represented by the letter A. The letter V denotes viral single-strand sequences. Sequences at the 5′ end of virion DNA are represented by the letter B. A dot denotes the leftmost *Pst*I site in the viral genome, and a prime symbol denotes the single *Xba*I site. The left end-to-left end bridge fragments which were inserted into the pUC vector are stippled, while the right end-to-right end bridge fragments are cross-hatched.

polymerase I as described by the supplier (Boehringer). Substrates for probe synthesis were as follows: (i) linearized pUC19 DNA; (ii) a gel-purified DNA fragment spanning the *Dpn*I-to-*Dpn*I-*Bam*HI sites at nucleotides 277 and 418 in pUC19; and (iii) a gel-purified DNA fragment spanning the *Hin*dIII-to-*Pvu*II sites at nucleotides 447 and 628 in pUC19.

DNA sequencing. Cloned MVM sequences were sequenced by chain termination from double-stranded templates with commercially available primers complementary to sequences in the pUC polylinker (1201 and 1211; New England Biolabs) and with modified bacteriophage T7 DNA polymerase marketed under the name Sequenase (U.S. Biochemical Corp., Cleveland, Ohio) in accordance with the manufacturer's directions.

RESULTS

Molecular cloning of concatemer junction fragments. Figure 1 shows the structure of MVM RF DNA and suggests how such a form could be generated by repeated rounds of self-priming, strand displacement synthesis, and hairpin formation at the 3′ terminus (44). Figure 1, step 1, shows the 3′-terminal palindrome of incoming virion DNA being used by a host polymerase to prime the synthesis of a complementary strand, giving rise to monomer duplex RF DNA which is covalently closed at the left end. During this process, the 5′ hairpin is displaced and copied to yield at the right end an "extended" terminus in which there are two complementary copies of the terminal palindrome. The 5′ terminus is then rearranged to form a rabbit-ear structure (step 2), providing the primer for strand displacement synthesis (step 3), thus giving rise to dimer RF (steps 4 and 5). Tetramer RF is generated by repeating these maneuvers (step 6).

The genome of MVM has unique termini. Fig. 1, step 6, shows the structure of tetramer RF and indicates the left-end viral 3′ junction (A in Fig. 1) and the right-end viral 5′ junction (B in Fig. 1) fragments which were cloned into plasmids pUC18 and pUC19 to yield clones pLEB-711 and pREB-1412, respectively. The structure of these clones was established by restriction mapping and partial sequencing.

Plasmids containing palindromic inserts assumed complex structures in vitro. When electrophoresed on neutral gels, these plasmid DNAs invariably resolved into multiple bands, as seen for plasmids pLEB-711 and pIP-304 in lanes 1 of Fig. 2A and B, respectively. This complex pattern is presumed to reflect secondary structure, since the same DNA preparations gave a vastly simplified pattern upon electrophoresis

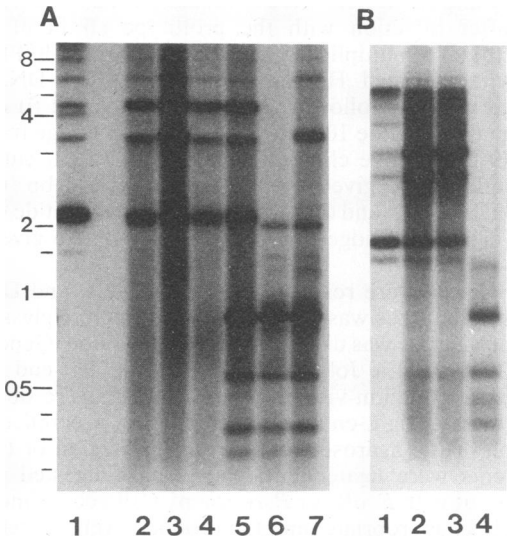

FIG. 2. (A) Southern transfer of a 1.4% neutral agarose gel probed with ^{32}P-labeled total pUC19 DNA, showing plasmid pLEB-711 before (lane 1) and after transfection into uninfected A9 cells (lanes 2, 4, and 6) or A9 cells superinfected with MVM (lanes 3, 5, and 7). Aliquots of total DNA recovered from the cells (lanes 2 and 3) were digested with restriction enzyme *Mbo*I (lanes 4 and 5) or *Dpn*I (lanes 6 and 7). (B) Similarly probed transfer, showing plasmid pIP-304 before (lane 1) and after (lanes 2 to 4) transfection into A9 cells superinfected with MVM. Aliquots of total DNA recovered from the cells (lane 2) were digested with *Mbo*I (lane 3) or *Dpn*I (lane 4). Positions of molecular weight standards are indicated on the left (1-kb ladder; Bethesda Research Laboratories).

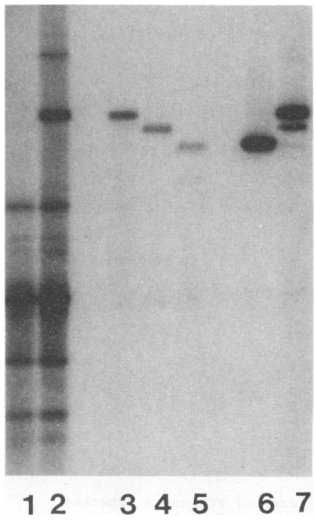

FIG. 3. Southern transfer of a 1.4% neutral agarose gel probed with ^{32}P-labeled total pUC19 DNA, showing the *Dpn*I digestion products of total pLEB-711 DNA recovered from uninfected cells (lane 1) and cells superinfected with MVM (lane 2). The major *Dpn*I-resistant DNA species from infected-cell DNA was gel purified and reelectrophoresed before (lane 3) and after being cut with *Hin*dIII (lane 4) or both *Hin*dIII and *Eco*RI (lane 5). For comparison, input pLEB-711 DNA was digested with *Eco*RI (lane 7) or *Eco*RI and *Hin*dIII (lane 6).

under denaturing conditions or after linearization. Cleavage with restriction enzymes which cut at one side of the viral insert gave two bands, a major form migrating at the expected position and a submolar form migrating just ahead of the linear form (e.g., Fig. 3, lane 7). Although we do not fully understand the structure of the submolar form, the fact that it disappeared upon electrophoresis at an alkaline pH suggests that it reflects secondary structure or perhaps the adoption of a cruciform structure by the insert. Similarly, cleavage with enzymes which excise the insert gave two forms of viral DNA, a form of the expected size and a submolar form approximately half this size (Fig. 4b, lane 2); the latter appeared to be self-annealed single-stranded DNA which had been extruded from the insert as part of the cruciform structure, since it too disappeared under alkaline conditions. Similar observations were made for all plasmids with palindromic inserts used in this study, not just those carrying the concatemer junction fragments. Thus, it seems likely that all of these plasmids present the viral sequences in both the linear and the cruciform configurations, at least in vitro.

In vivo resolution and replication of the bridge plasmids. To test whether the cloned bridge fragments could be recognized by *trans*-acting viral enzymes, we transfected the circular plasmids into permissive murine cells and superinfected the cells with MVM. Plasmid DNA recovered from uninfected control cells was resistant to digestion with *Mbo*I (Fig. 2A, lane 4) but could be digested to completion with *Dpn*I (Fig. 2A, lane 6), indicating that it still carried the bacterial methylation pattern and had not replicated in transfected cells. In contrast, plasmid DNA recovered from cells superinfected with MVM(p) contained two populations of molecules, some which remained sensitive to *Dpn*I digestion and which were thus of bacterial origin and some which were insensitive to digestion with *Dpn*I (Fig. 2A, lane 7). These resistant molecules migrated at about 3.4 and 6.8 kb on neutral agarose gels, suggesting that they might be linear monomeric and dimeric forms of the input plasmid (Fig. 2A, lane 7). DNA which had been resolved but not replicated would be expected to yield new *Dpn*I digestion products not seen in digests of the original, bacterially synthesized plasmid preparation, but such forms were not apparent. Although much of the DNA recovered from infected cells was resistant to *Mbo*I digestion, a significant fraction was cleaved, yielding a series of digestion products which appeared similar to those obtained by *Dpn*I digestion of the unreplicated input plasmid (Fig. 2A, cf. lane 5 with lanes 6 and 7). Since *Mbo*I cannot cleave DNA which is either methylated or hemimethylated at its restriction site, both strands of the susceptible molecules must have been replicated in the eukaryotic cells. Similar results were obtained with clone pREB-1412, containing the right-end bridge fragment (see below). However, when clone pIP-304 or a variety of other clones containing palindromic arrangements of MVM sequences not associated with the bridge regions were transfected and the cells were superinfected with MVM, the constructs were not resolved or replicated (Fig. 2B). Since pIP-304 contains a perfect 304-base palindrome derived from clone pLEB-711 by deletion of the internal *Nco*I bridge fragment, it is able to form a cruciform structure similar to those formed by the bridge fragment clones. Failure to resolve such DNA indicates that the ability of the substrate to adopt a cruciform structure per se is insufficient to allow viral *trans*-acting factors to initiate replication. Thus, both the right-hand and the left-hand concatemer bridge fragments of MVM must contain origins of DNA replication which can be accessed in virally infected but not uninfected cells.

The extent to which the plasmid sequences were replicated in infected cells varied from transfection to transfection, especially when calcium phosphate precipitates were used to deliver the DNA. In more recent experiments, we have chosen to use lipofectin for transfection (22). Although the levels of resolution and replication were lower than the best results seen with calcium phosphate, the procedure was much more reproducible. We presume that to be resolved and replicated, the plasmid DNA must reach the nucleus of the host cell, and it may be that much of the unreplicated DNA seen in Fig. 2 is in some other cellular compartment.

Plasmids are replicated as linear molecules with viral sequences at both termini. To examine the structure of the transfected, replicated DNA, we digested pLEB-711 DNA recovered from virally superinfected cells with *Dpn*I (Fig. 3, lane 2) and gel purified the major 3.4-kb *Dpn*I-resistant band (Fig. 3, lane 3), which comigrates with monomeric linear plasmid DNA (Fig. 3, lane 7). We digested this material with *Hin*dIII, which cuts in the pUC polylinker on one side of the viral insert. The product of this digestion (Fig. 3, lane 4) migrated as a discrete band with a mobility which was approximately halfway between that of linearized pLEB-711 (lane 7) and linear vector DNA (lane 6). Further digestion with *Eco*RI, which cuts in the pUC polylinker on the other side of the viral insert, gave a product (Fig. 3, lane 5) which comigrated with the linear vector DNA (lane 6). Thus, in vivo, plasmid DNA becomes linearized within the viral sequences and is replicated as a linear chromosome with viral telomeres. However, unlike the MVM genome, which has unique termini, the structures shown here have identical ends derived from the same end of the viral genome, in this case the left end.

When the DNA recovered from infected cells was digested

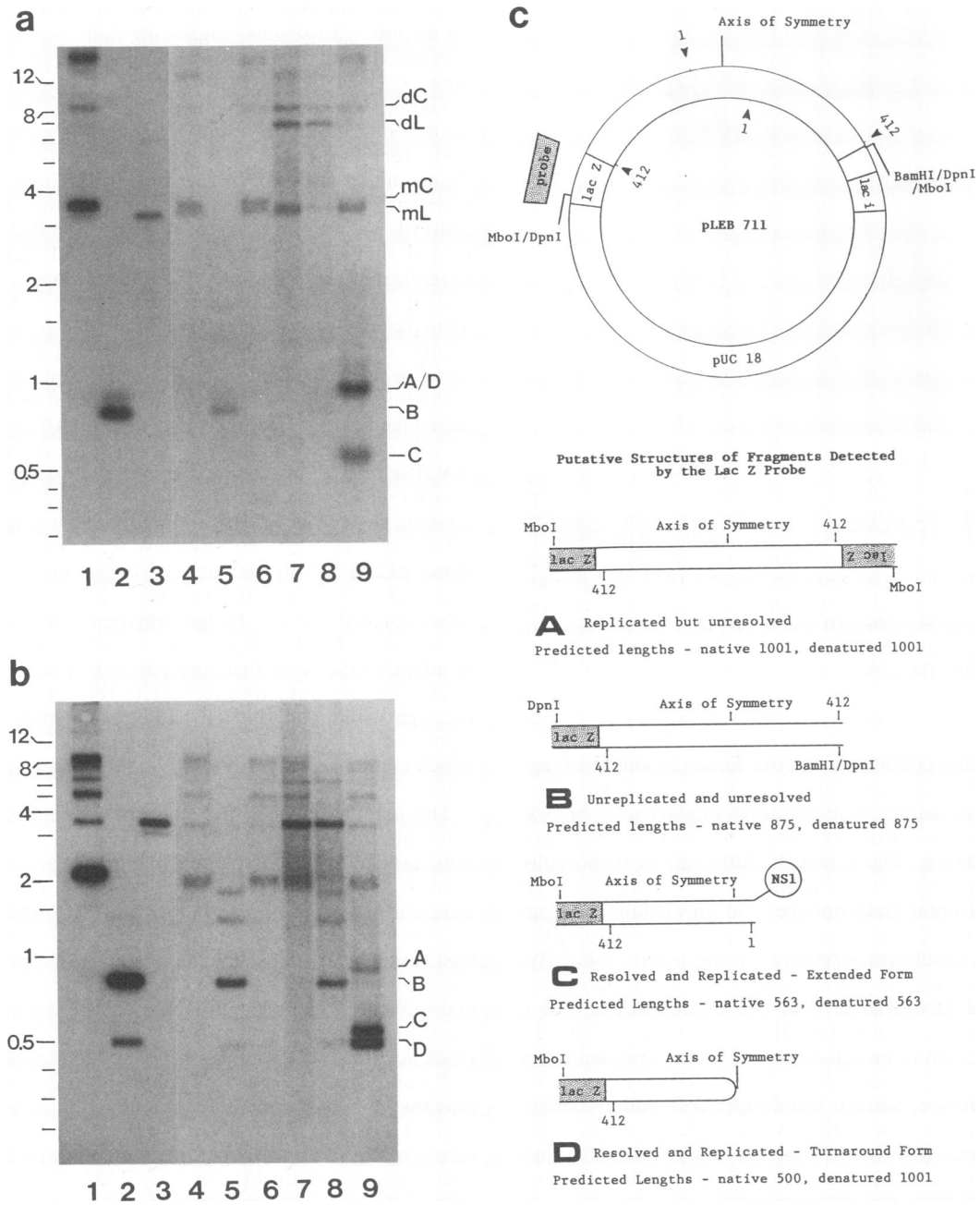

FIG. 4. Southern transfers of alkaline (a) or neutral (b) 1.4% agarose gels probed with a ^{32}P-labeled *Dpn*I fragment from the *lacZ* region of pUC19 DNA (nucleotides 217 and 418), which abuts and is continuous with one side of the viral insert in plasmid pLEB-711 (as indicated in panel 4c). In both panels a and b, input plasmid pLEB-711 DNA (lane 1) is shown following digestion with *Dpn*I (lane 2) or *Eco*RI (lane 3). Samples of total DNA recovered from uninfected cells (lanes 4 to 6) or cells superinfected with MVM (lanes 7 to 9) either were left undigested (lanes 4 and 7) or were digested with *Dpn*I (lanes 5 and 8) or *Mbo*I (lanes 6 and 9). Positions of molecular weight standards are shown (1-kb ladder; Bethesda Research Laboratories). mC, monomer circular form; mL, monomer linear form; dC, dimer circular form; dL, dimer linear form. Fragments A thru D are *Dpn*I or *Mbo*I digestion products detected with this probe. (c) Structure of pLEB-711 and position of the *lacZ* probe. The putative structures of the *Dpn*I and *Mbo*I digestion products (fragments A to D) seen in panels a and b are depicted, together with their calculated lengths. Structure A is the *lacZ-lacZ* junction fragment present in one of the predicted dimer forms of the replicating linear molecule prior to its further resolution to two monomer forms. The other form of junction fragment, with two *lac*i arms, would not be detected with the *lacZ* probe used and would be separated from the *lac*i sequence by *Mbo*I digestion.

to completion with *Dpn*I to fragment all unreplicated DNA and the remaining high-molecular-weight forms were compared following electrophoresis on both native and denaturing (alkaline) agarose gels, the newly replicated molecules were seen to resolve into multiple forms (cf. Fig. 4a, lane 8, with Fig. 4b, lane 8, noting that the *Dpn*I fragments seen in these blots appear different from those seen previously because the probe has been restricted to a 141-base junction

sequence). In the alkaline gel (Fig. 4a), two major species comigrated with markers at about 7 and 9 to 10 kb. The predominant 7-kb form migrated at 3.4 kb under nondenaturing conditions (as in Fig. 4b, lane 8, and as confirmed by two-dimensional electrophoresis in neutral and then alkaline gels) and represented dimeric linear plasmid molecules. The other major, newly replicated form (9 to 10 kb) also migrated at 3.4 kb under neutral conditions and appeared to contain circular (covalently closed) dimeric molecules (these were also present in the input plasmid; Fig. 4a, lane 1). Relatively little of the in vivo replicated DNA comigrated with unit-length linearized plasmid molecules (Fig. 4a, lane 3). These same high-molecular-weight *Dpn*I-resistant forms did not predominate in plasmid DNA recovered from uninfected cells (Fig. 4a, lane 4); the latter DNA mostly migrated as circular and linear monomeric forms. Since we know that the newly replicated, unit-length, duplex DNA molecules seen under nondenaturing conditions have viral sequences at their termini (Fig. 3), the results suggest that they are made up of molecules in which the two strands of the duplex have become covalently continuous at one or both viral telomeres.

Structure of the resolved and replicated termini. (i) Left-end (viral 3′-to-3′) bridges yield "turn-around" and "extended" termini. To analyze the newly replicated termini of the left-end bridge clone pLEB-711 in more detail, we probed digests with a small (141-base) *Dpn*I fragment of pUC DNA (indicated in Fig. 4c) which lies between the *Dpn*I site at nucleotide 277 and the *Dpn*I-*Bam*HI site at nucleotide 418 in the vector and which consequently abuts one side of the viral insert. Since there are no *Dpn*I-*Mbo*I sites within the pLEB-711 insert, this probe detects the *Dpn*I-*Mbo*I fragment containing the intact viral palindrome in unresolved DNA but only one side of this palindrome when the viral sequences have been resolved. With this probe (Fig. 4a and b), we found that *Dpn*I digestion of input plasmid DNA (lanes 2 in Fig. 4a and b) yielded a major band (band B) at about 875 bp representing the unresolved MVM insert and the expected, submolar product of half this size seen only in neutral gels and discussed previously. These forms were also seen in *Dpn*I digests of DNA recovered from both uninfected (lanes 5 in Fig. 4a and b) and MVM-superinfected (lanes 8 in Fig. 4a and b) cells. Additional submolar bands with higher molecular weights (at 1.5 and 1.8 kb in Fig. 4b) in all of these lanes were partial digestion products.

In contrast, the *Mbo*I digestion products of in vivo resolved and replicated DNA lacked the major 875-bp band, but this was replaced with three new species seen on the neutral gel (Fig. 4b, lane 9), a minor band (band A) of about 1,000 bp and two major bands (bands C and D) of about 550 and 500 bp. Figure 4c shows the probable structures of these fragments as deduced from all of the experimental data presented in this paper. These structures suggest that bands A, C, and D are 1,001, 563, and 500 bp, respectively. When similar digests were denatured and resolved on an alkaline gel, the *Mbo*I products (Fig. 4a, lane 9) migrated as two major bands of 1,001 and 563 nucleotides.

Two-dimensional gel electrophoresis (Fig. 5) showed that under alkaline conditions, both the 500- and the 1,001-bp bands from the neutral dimension (bands D and A, respectively) migrated as a 1,001-base linear form, while the 563-bp band (band C) migrated at the same position in both gels. These results indicate that the 875-bp *Dpn*I fragment from the input plasmid which is detected with this probe was resolved (and replicated) in vivo to give three forms. The first form is a covalently closed turn-around molecule with a copy of the 141-base plasmid sequence from the *lacZ* region on both strands. This molecule gives a 500-bp duplex which is 1,001 bases long under denaturing conditions (structure D in Fig. 4c). The second, and relatively minor, form (structure A in Fig. 4c) is a palindromic duplex copy of fragment D which is presumed to derive from a newly replicated molecule awaiting further resolution. The third form (structure C in Fig. 4c) is an extended molecule of 563 bp in which the two DNA strands are not covalently linked but are both about 60 nucleotides longer than would be obtained were the palindrome simply nicked at its axis of dyad symmetry. These molecules presumably contain the complete viral palindrome, having been resolved at a specific resolution site on one side of the axis of symmetry. Similar extended and turn-around termini are characteristically found at the ends of duplex RF MVM DNA during the course of a normal infection (10, 48), and thus in vivo resolution of the concatemer junction plasmids appears to mimic the normal cleavage process. It should be noted that the two arms of the viral palindrome are slightly asymmetric but that the *Dpn*I probe used in these experiments only detects one of the two virus-plasmid junction fragments (Fig. 4c), so the same half of the input palindrome is replicated to give both extended and turn-around forms.

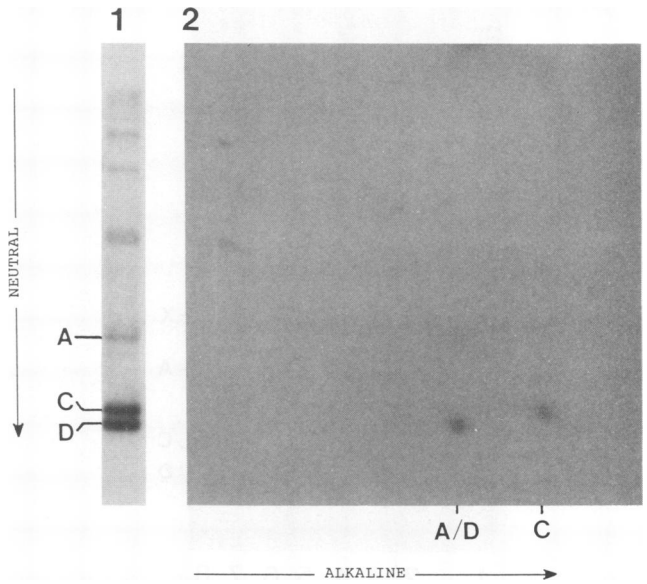

FIG. 5. Southern transfer of a two-dimensional 1.4% agarose gel probed with the ^{32}P-labeled *Dpn*I fragment from the *lacZ* region of pUC DNA (nucleotides 217 to 418) shown in Fig. 4c. Total DNA recovered from A9 cells transfected with pLEB-711 and superinfected with MVM was digested with *Mbo*I, and the products were electrophoresed on a neutral agarose gel (lane 1). An exactly comparable lane from the same gel was excised and inserted into a depression along the top of an alkaline gel and reelectrophoresed (lane 2), together with a separate lane of molecular weight markers. As shown in Fig. 4C, fragments A and D in the neutral gel migrated in the alkaline gel as fragments of about 1,001 bases, while fragment C migrated as a 563-base fragment in both dimensions.

(ii) NS-1 is associated with all extended termini. When the viral genome is replicated during infection, a copy of the virally encoded nonstructural protein NS-1 becomes covalently attached to the 5′ termini of both viral and complementary strands and to all single-stranded progeny DNA (14). If in vivo replication of the bridge plasmids recapitu-

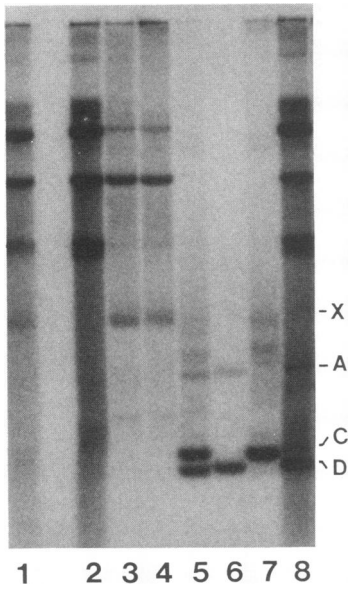

FIG. 6. Southern transfer of a neutral 1.4% agarose gel probed with the ^{32}P-labeled *Dpn*I fragment from the *lacZ* region of pUC DNA (nucleotides 217 to 418) shown in Fig. 4c. Samples of total DNA recovered from A9 cells transfected with pLEB-711 and superinfected with MVM (lane 1) were disrupted in SDS and immunoprecipitated with antiserum directed against the amino-terminal peptide of NS-1 (lanes 3 to 7). NS-1-associated pLEB-711 DNA was either left undigested (lane 3) or digested with *Dpn*I (lane 4) or *Mbo*I (lane 5). An *Mbo*I-digested immunoprecipitate exactly comparable to that seen in lane 5 was separated by centrifugation into an NS-1-associated pellet fraction (lane 7) and a free supernatant fraction (lane 6). Material left in the unbound fractions immediately following immunoprecipitation with anti-NS-1 serum (lane 2) was also subsequently digested with *Mbo*I (lane 8). Fragments A, C, and D, as discussed in Fig. 4, are indicated. A diffuse *Dpn*I-resistant and *Mbo*I-sensitive band present in the immunoprecipitated DNA is marked X. This band is of unknown origin and structure but it is unlikely to be single-stranded progeny DNA since most of it appears to be digested with *Mbo*I and it cannot be precipitated with anti-capsid serum from nondenatured extracts.

lates this process, then the resolved and replicated plasmid DNA should show a characteristic pattern of NS-1 association. Figure 6 shows the results of a series of immunoprecipitations carried out with antiserum directed against the amino-terminal domain of NS-1. Prior to precipitation, proteins in the cell extracts were extensively denatured and dissociated by being heated to 60°C for 30 min in 2% SDS to ensure that only covalently associated DNA would remain attached to the nonstructural protein. Under these conditions, immunoprecipitation selected a subpopulation of plasmid DNA (Fig. 6, lane 3) from the total infected-cell extract (lane 1), leaving most of the plasmid molecules in the unbound fraction (lane 2). However, the selected DNA was totally resistant to cleavage by *Dpn*I (lane 4) and fully susceptible to cleavage by *Mbo*I (lane 5), showing that NS-1 was specifically associated with in vivo replicated plasmid molecules. After digestion with *Mbo*I, a similar immunoprecipitate was recentrifuged to separate DNA fragments which were directly attached to NS-1 molecules (and thus remained associated with the pellet; Fig. 6, lane 7) from those which were released into the supernatant (Fig. 6, lane 6). Under these conditions, the 500- and 1,001-bp fragments were released from the precipitate, while the 563-bp fragment remained covalently associated with NS-1 molecules in the pellet (Fig. 6, lane 7). This pattern of association mimics that seen during an MVM infection, in which only extended RF termini are associated with NS-1, and so confirms that NS-1 is involved in the resolution of the bridge plasmids in vivo.

However, since NS-1 is only associated with termini in the extended configuration, putative dimeric circular forms of *Dpn*I-resistant DNA (such as those seen migrating at about 9 to 10 kb in Fig. 4a, lane 8) should not be precipitated with anti-NS-1 serum. Figure 6, lane 8, shows the *Mbo*I cleavage products of the unbound material from an anti-NS-1 serum precipitation. Since immunoprecipitation is rarely quantitative, a small proportion of the DNA present in this fraction may still be NS-1 associated and give rise to the typical digestion products just discussed. However, most of this DNA is free of NS-1, yet it clearly contains newly replicated plasmid DNA. Moreover, the vast majority of the termini generated by *Mbo*I digestion are in the covalently closed turn-around configuration (Fig. 6, cf. lane 8 with lanes 5, 6, and 7), suggesting that they are derived from molecules in which the two DNA strands of the plasmid have become covalently continuous. This observation suggests that the resolution of the left-end junction clone involves both a cutting step and a ligation step and supports the idea that this end of the genome is cleaved in a topoisomeraselike reaction (1) rather than by the simple introduction of a single-strand nick. We have previously found evidence for a similar ligation step during the replication of MVM DNA in a normal, lytic infection (10), again suggesting that the resolution of the bridge clones in vivo involves authentic viral and cellular components.

For clarity, the analyses presented thus far have all involved the *lacZ*-virus junction of plasmid pLEB-711, but similar NS-1-associated extended and covalently closed turn-around termini are also generated from plasmids with junction fragments ranging from 157 (pLEB-157) to 2,049 (pLEB-2049) bp (data not shown) and from both sides of the viral insert. Since *Dpn*I-*Mbo*I digestion cleaves between the plasmid and viral sequences at the *Bam*HI site of the pUC18 polylinker, we cannot use probes derived from vector DNA in conjunction with these enzymes to distinguish between replicated and input pLEB-711 DNAs. However, *Pvu*II digestion of the recovered DNA excises a 1,032-bp fragment which spans plasmid sequences on both sides of the pUC polylinker and the intervening viral palindrome (Fig. 7b). Resolution of either arm of the viral DNA can then be monitored by probing with plasmid sequences from the appropriate *Pvu*II site to the polylinker. Figure 7a, lanes 1 to 6, shows such an analysis with the *Pvu*II-to-*Hin*dIII fragment probe (Fig. 7b), which monitors the resolution of the viral arm previously undetected by the *lacZ* fragment probe. To enrich for newly replicated DNA, we carried out immunoprecipitation with anti-NS-1 serum (Fig. 7a, lane 3) using a somewhat less rigorous washing procedure than that used in the previous experiment, cleaved the precipitated DNA with *Pvu*II (lane 4), and separated the digestion products into NS-1-associated (lane 5) and released (lane 6) fragments. Although in this case, the immunoprecipitates were relatively contaminated with unreplicated plasmid DNA, *Pvu*II digestion readily separated the resolved extended and turn-around DNA fragments (of 623 and 458 bp, respectively, as calculated from the structures depicted in Fig. 7b) from the unresolved 1,032-bp plasmid sequence. Once again, the higher-molecular-weight extended molecules were complexed with NS-1, while the lower-molecular-weight turn-around molecules were not.

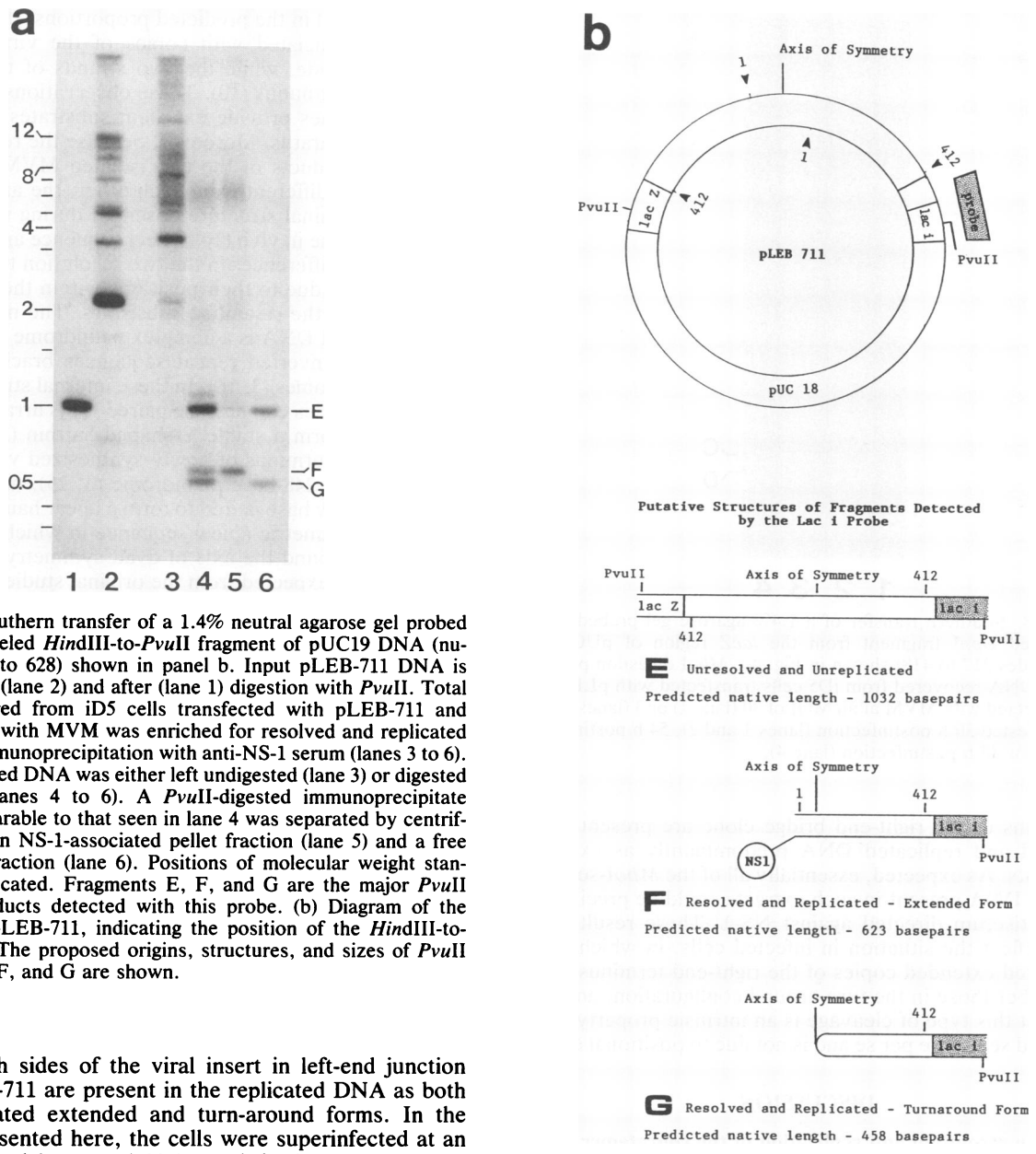

FIG. 7. Southern transfer of a 1.4% neutral agarose gel probed with a ^{32}P-labeled *Hin*dIII-to-*Pvu*II fragment of pUC19 DNA (nucleotides 447 to 628) shown in panel b. Input pLEB-711 DNA is shown before (lane 2) and after (lane 1) digestion with *Pvu*II. Total DNA recovered from iD5 cells transfected with pLEB-711 and superinfected with MVM was enriched for resolved and replicated species by immunoprecipitation with anti-NS-1 serum (lanes 3 to 6). The precipitated DNA was either left undigested (lane 3) or digested with *Pvu*II (lanes 4 to 6). A *Pvu*II-digested immunoprecipitate exactly comparable to that seen in lane 4 was separated by centrifugation into an NS-1-associated pellet fraction (lane 5) and a free supernatant fraction (lane 6). Positions of molecular weight standards are indicated. Fragments E, F, and G are the major *Pvu*II digestion products detected with this probe. (b) Diagram of the structure of pLEB-711, indicating the position of the *Hin*dIII-to-*Pvu*II probe. The proposed origins, structures, and sizes of *Pvu*II fragments E, F, and G are shown.

Thus, both sides of the viral insert in left-end junction clone pLEB-711 are present in the replicated DNA as both NS-1-associated extended and turn-around forms. In the analyses presented here, the cells were superinfected at an MOI of 30 and harvested 30 h postinfection. Under these conditions, the two forms were present in approximately equimolar amounts or with the turn-around form slightly predominating. When samples were harvested at earlier times postinfection, the same proportions were observed, while when they were harvested over an extended period, the turn-around form eventually predominated. Thus, in an experiment in which the cells were infected at an MOI of 3, by 30 h postinfection the two forms were present in approximately equimolar amounts (Fig. 8, lane 2), by 54 h postinfection turn-around form predominated (lane 3), and by 80 h postinfection they accounted for about 90% of the resolved and replicated termini (lane 4). Thus, with the left-end junction clones, the generation of resolved and replicated termini in the turn-around configuration is not a minor or trivial event; it is the major consequence of this procedure.

(iii) Right-end (viral 5′-to-5′) bridges yield predominantly extended termini. Superinfection of cells transfected with the right-end bridge clones gave relatively simple results compared with those obtained with the left-end bridge clones. When pREB-1412 was transfected into iD5 cells, it was resolved and replicated provided the cells were superinfected with MVM, but most of the *Dpn*I-resistant DNA migrated as linear monomeric plasmid molecules when analyzed on either neutral or denaturing gels (data not shown). When this DNA was immunoprecipitated with anti-NS-1 serum (Fig. 9a, lane 3) and the crude precipitates were analyzed after *Pvu*II digestion with a probe derived from the *lac*i region of the vector (Fig. 9b) as described above, this arm of the palindrome was found to be present in the resolved DNA predominantly as NS-1-associated extended forms (Fig. 9a, lanes 4, 5, and 6). When these blots were reprobed with a plasmid sequence from the other side of the polylinker (in this case from the *Pvu*II site at nucleotide 306 in pUC19 to the polylinker *Eco*RI site at nucleotide 396), the same results were obtained (data not shown), indicating that

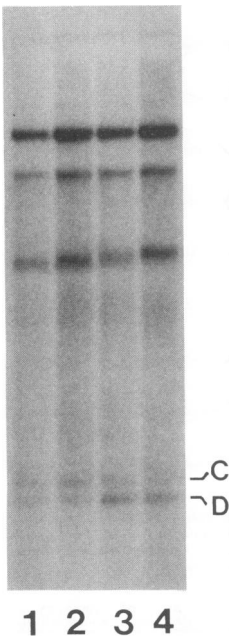

FIG. 8. Southern transfer of a 1.4% agarose gel probed with a ^{32}P-labeled *Dpn*I fragment from the *lacZ* region of pUC DNA (nucleotides 217 to 418) shown in Fig. 4c. *Mbo*I digestion products of total DNA recovered from iD5 cells transfected with pLEB-711, superinfected with MVM at an MOI of 30 (lane 1) or 3 (lanes 2 to 4), and harvested 30 h postinfection (lanes 1 and 2), 54 h postinfection (lane 3), or 80 h postinfection (lane 4).

both arms of the right-end bridge clone are present in the resolved and replicated DNA predominantly as extended fragments. As expected, essentially all of the *Mbo*I-sensitive plasmid DNA present in such extracts could be precipitated with antiserum directed against NS-1. These results once again reflect the situation in infected cells, in which NS-1-associated extended copies of the right-end terminus vastly outnumber those in the turn-around configuration, and indicate that this type of cleavage is an intrinsic property of the right-end sequence per se and is not due to positional effects.

DISCUSSION

In vivo resolution and replication of the concatemer bridge plasmids. We have shown that the duplex palindromic junction fragments spanning both the viral 5′-to-5′ and the viral 3′-to-3′ bridges in concatemeric MVM RF DNA can be resolved and replicated in superinfected cells when delivered as part of a circular *E. coli* plasmid. Under these conditions, the viral sequences in some of the input plasmid molecules are resolved and the plasmids replicate as linear structures with viral sequences at both termini. Similar studies with poxvirus telomeres (16, 29, 31–33) and isolated fragments of herpesvirus DNA (41) have proven invaluable in permitting the identification and dissection of *cis*-acting sequences responsible for many aspects of viral DNA replication, such as terminal resolution, DNA amplification, and packaging, even though authentic in vitro systems for many of these complex processes remain intractable.

The resolution of each cloned MVM junction fragment in vivo appears analogous to that observed at the corresponding viral telomere during infection. The termini generated include both extended and turn-around forms of the predicted sizes and in the predicted proportions; the former are covalently associated with copies of the virally encoded NS-1 polypeptide, while the two strands of the latter are covalently continuous (10). These observations suggest that the bridge clones provide excellent substrates for the viral resolution apparatus. Moreover, because the resolution and replication products of the two isolated MVM termini are quantitatively different from each other, the analogous disparities in terminal structure observed during replication of the viral genome in vivo (10) reflect sequence and/or secondary structure differences in the two resolution templates and are not simply due to their positions within the genome.

Structure of the resolution substrates. The mature 3′ terminus of MVM DNA is a complex palindrome in which two 26-nucleotide inverted repeat sequences bracket a pair of shorter palindromes (3, 18). In these internal structures 54 of the 67 nucleotides can be base paired. This arrangement can be folded to form a stable Y-shaped hairpin (3). Similarly, the mature 5′ terminus of newly synthesized virion DNA is known to be a 248-base palindrome (3, 15), most of which can be perfectly base paired to form a linear hairpin, but with a slightly asymmetric apical sequence in which 40 of the 46 nucleotides around the axis of dyad symmetry can be base paired (3). As expected from the original studies of concatemer structure (48), the MVM concatemer junction fragments analyzed in this study were found to be palindromes in which a single copy of the appropriate asymmetric apical sequence was flanked by perfectly base-paired head-to-head (3′-to-3′) or tail-to-tail (5′-to-5′) copies of the viral genome. In vitro, the plasmids carrying these constructs appeared to adopt many different configurations, as judged by the number of distinct bands resolved upon electrophoresis on neutral agarose gels. The secondary and tertiary structures of plasmids carrying analogous poxvirus palindromes have been studied in some detail (17, 30). In vitro, these plasmids extrude cruciform structures which map to the central axis of the viral repeat sequence, and although no steady-state pool of structures in the extruded cruciform configuration could be identified in *E. coli* (17), its transient presence in vivo was deduced from the presence of a major deletion variant generated even in some recombination-deficient strains of *E. coli*.

Since the MVM junction clones appear to behave in a similar manner, it seems likely that the viral sequences are presented to the replication machinery of transfected cells both in a linear duplex configuration and as extruded hairpin structures. Such a presentation is potentially useful for an in vitro replication substrate, since it mimics both situations prevailing during infection, in which fully base-paired duplex bridge fragments and hairpin terminal structures are present. At present we do not know which forms of each terminus are metabolically active in vivo. Indeed, one current replication model (1) suggests that the processing machinery shows an absolute requirement for the duplex bridge form of the left-hand viral terminus, while the right-hand viral terminus might be preferred in the hairpin configuration (1, 13). Further analysis of asymmetric deletion mutants of the bridge clones may clarify these requirements, but at present we cannot draw conclusions about the in vivo structure of the templates.

Structure of the resolution products. In this paper we provide direct evidence that, although disparate in sequence, both of the MVM terminal palindromes contain latent origins of DNA replication which can be activated by viral *trans*-acting factors in vivo. Sequences and/or structures at the right end of the genome allow this terminus to be resolved

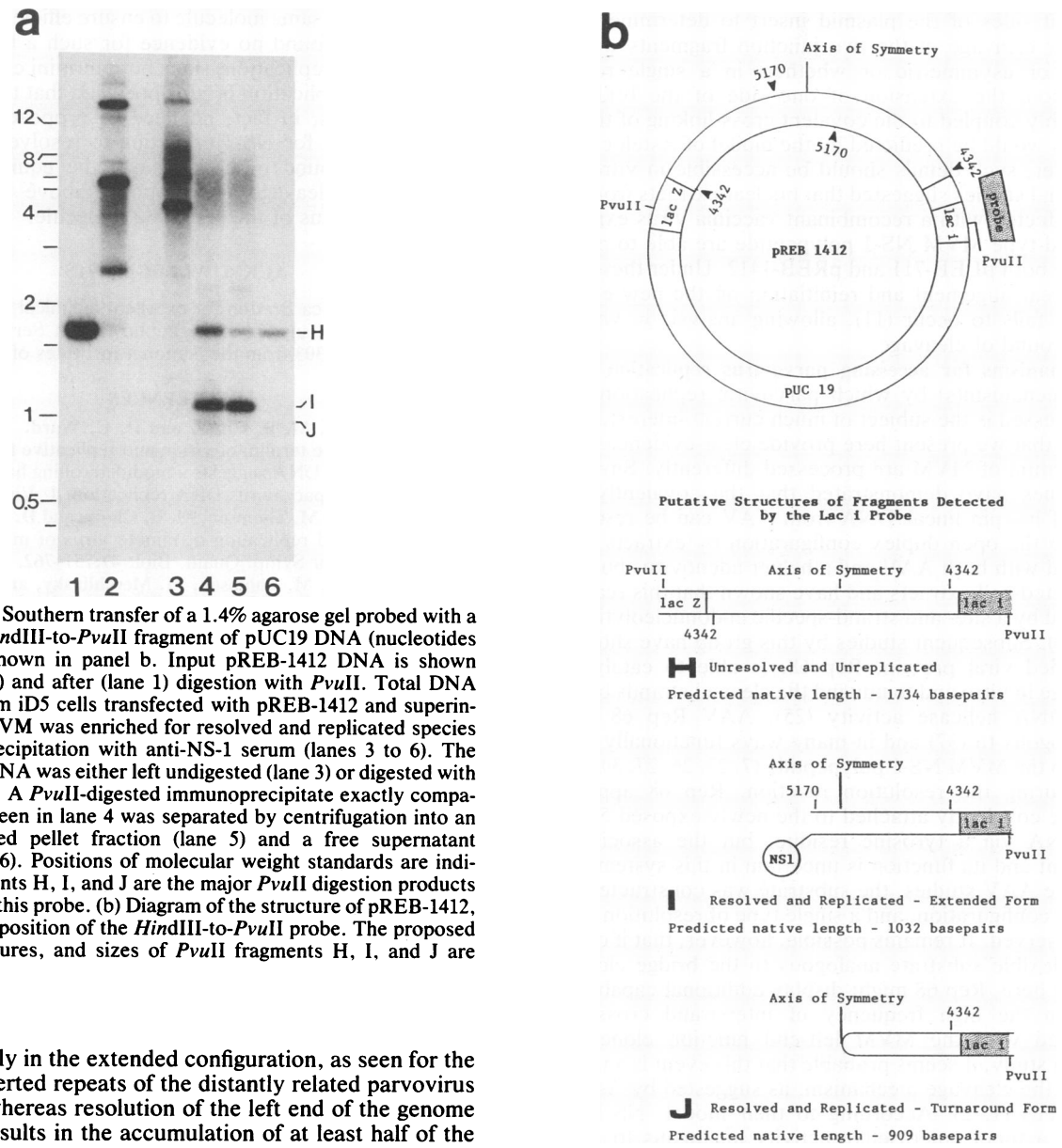

FIG. 9. (a) Southern transfer of a 1.4% agarose gel probed with a ^{32}P-labeled *Hin*dIII-to-*Pvu*II fragment of pUC19 DNA (nucleotides 447 to 628) shown in panel b. Input pREB-1412 DNA is shown before (lane 2) and after (lane 1) digestion with *Pvu*II. Total DNA recovered from iD5 cells transfected with pREB-1412 and superinfected with MVM was enriched for resolved and replicated species by immunoprecipitation with anti-NS-1 serum (lanes 3 to 6). The precipitated DNA was either left undigested (lane 3) or digested with *Pvu*II (lane 4). A *Pvu*II-digested immunoprecipitate exactly comparable to that seen in lane 4 was separated by centrifugation into an NS-1-associated pellet fraction (lane 5) and a free supernatant fraction (lane 6). Positions of molecular weight standards are indicated. Fragments H, I, and J are the major *Pvu*II digestion products detected with this probe. (b) Diagram of the structure of pREB-1412, indicating the position of the *Hin*dIII-to-*Pvu*II probe. The proposed origins, structures, and sizes of *Pvu*II fragments H, I, and J are shown.

predominantly in the extended configuration, as seen for the identical inverted repeats of the distantly related parvovirus AAV (40), whereas resolution of the left end of the genome invariably results in the accumulation of at least half of the termini in the covalently closed turn-around configuration. While it is possible to explain the generation of a turn-around form on one end of a duplex molecule simply as the result of initiating replication at that end by hairpin priming, it is not possible to explain the existence of turn-around structures on both ends of the same molecule by the simple hairpin resolution mechanism documented for AAV (4, 5, 40). This problem persists even if differences in the rate constants for nicking on the two sides of the bridge, as suggested by Chen and colleagues (9), are assumed. In contrast, if we assume that resolution of the left-end bridge proceeds by the linked nicking and ligating mechanism proposed by Astell et al. (1), half of the ends would be generated initially in the turn-around configuration. In this case, the subsequent round of replication would proceed through a dimeric intermediate, generating two progeny plasmid molecules, one with both ends in the extended configuration and the other with both ends in the turn-around configuration. The latter type of molecule would be a replication endpoint, since its hairpin termini could not be resolved by exclusively duplex bridge resolution. Such a mechanism would predict the progressive accumulation of covalently closed termini over time, and this phenomenon is documented for transfected left-end bridges in Fig. 8. Although such forms might also accumulate with time in vivo by a mechanism(s) unrelated to the actual processes used to resolve the viral termini, this explanation seems unlikely because similar forms were not generated from the right-end bridge clone under identical conditions. Indeed, the relatively low frequency of such covalently closed molecules among the resolution products of pREB-1412 suggests that turn-around forms of the right end are efficiently resolved. Whether they can also be cleaved from the duplex bridge structure or whether they absolutely require this substrate to adopt a cruciform configuration remains to be determined.

Since resolution and replication were closely linked in vivo, we were not able to use single-stranded probes from

different sides of the plasmid insert to determine directly whether cleavage of the two junction fragments was symmetric or asymmetric or whether, in a single round of resolution, the extension of one side of the bridge was invariably coupled to the covalent cross-linking of the other side, as would be predicted by the model of Astell et al. (1). However, such details should be accessible in vitro, since our initial studies suggested that nuclear extracts from HeLa cells infected with a recombinant vaccinia virus expressing the wild-type MVM NS-1 polypeptide are able to nick and resolve both pLEB-711 and pREB-1412. Under these conditions, rearrangement and reinitiation off the new extended termini fails to occur (11), allowing analysis in vitro of a single round of cleavage.

Mechanisms for accessing parvovirus replication origins. The mechanism(s) by which parvoviral replication origins are accessed is the subject of much current interest, and the results that we present here provide clear evidence that the two termini of MVM are processed differently. Snyder and colleagues have demonstrated that the covalently joined ends of hairpin linear DNA from AAV can be resolved in vitro to the open duplex configuration by extracts of cells infected with both AAV and a helper adenovirus but not by uninfected-cell extracts and have shown that this reaction is initiated by a site- and strand-specific endonucleolytic cleavage (40). Subsequent studies by this group have shown that a purified viral protein, Rep 68, is able to catalyze this cleavage in vitro and to unwind the cleaved strands by virtue of a DNA helicase activity (25). AAV Rep 68 is both homologous to (37) and in many ways functionally comparable to the MVM NS-1 polypeptide (7, 23, 26, 27, 34, 35, 45, 46). During the resolution reaction, Rep 68 appears to become covalently attached to the newly exposed 5′ end of the DNA via a tyrosine residue, but the association is transient and its function is uncertain in this system (39).

In the AAV studies, the substrate was constructed in the hairpin configuration, and a single type of resolution activity was observed. It remains possible, however, that if offered a more flexible substrate analogous to the bridge clones described here, Rep 68 might display additional capabilities.

Given the high frequency of interstrand cross-linking observed with the MVM left-end junction clone in the present study, it seems probable that this event is an integral part of the cleavage mechanism, as suggested by Astell and colleagues (1, 2). According to their model, NS-1 would exhibit a topoisomeraselike activity analogous to that described for the phage ϕX174 gene A protein (19, 20). In this scheme, resolution starts with the introduction of one site-specific single-strand nick at which the NS-1 polypeptide is covalently joined to the 5′ end produced. Replication would initiate at the 3′ hydroxyl of this nick, progress across the palindrome, and then be terminated at the mirror-image cleavage site by NS-1 exchanging itself across analogous phosphodiester bonds. This process would result in the creation of an unreplicated turn-around terminus and an extended terminus, containing a newly synthesized viral sense strand at its 3′ end, and with NS-1 attached to the 5′ end of its complementary strand. Such a mechanism would explain the observed resolution products of the left end-to-left end junction of MVM and would readily explain the retention of the protein on the 5′ end of the cleaved strand and the use of relatively mobile, tyrosine-phosphate linkages between the DNA and the protein (14).

The observation that the two termini appear to be resolved differently suggests that they may perform fundamentally different functions and therefore that both ends may be required on the same molecule to ensure efficient replication. However, we found no evidence for such a hypothesis, at least for DNA replication, since both termini can function as independent replication origins provided that they are duplicated. There is, in fact, no need to propose an alternate mode of action for NS-1 operating to resolve a covalently closed turn-around terminus, since the equivalent of the mirror-image cleavage site proposed above would be the physical terminus of the resolving molecule.

ACKNOWLEDGMENTS

We thank Jessica Bratton for excellent technical assistance.

This work was supported by Public Health Service grants AI-26109 and CA-29303 from the National Institutes of Health.

REFERENCES

1. **Astell, C. R., M. B. Chow, and D. C. Ward.** 1985. Sequence analysis of the termini of virion and replicative forms of minute virus of mice DNA suggests a modified rolling hairpin model for autonomous parvovirus DNA replication. J. Virol. **54**:171–177.
2. **Astell, C. R., M. Thomson, M. B. Chow, and D. C. Ward.** 1983. Structure and replication of minute virus of mice DNA. Cold Spring Harbor Symp. Quant. Biol. **47**:751–762.
3. **Astell, C. R., M. Thomson, M. Merchlinsky, and D. C. Ward.** 1983. The complete DNA sequence of minute virus of mice, an autonomous parvovirus. Nucleic Acids Res. **11**:999–1018.
4. **Berns, K. I.** 1990. Parvovirus replication. Microbiol. Rev. **54**:316–329.
5. **Berns, K. I., and W. W. Hauswirth.** 1979. Adeno-associated viruses. Adv. Virus Res. **25**:407–432.
6. **Boissy, R., and C. R. Astell.** 1985. An Escherichia coli recBCs-bcBrecF host permits the deletion-resistant propagation of plasmid clones containing the 5′-terminal palindrome of minute virus of mice. Gene **35**:179–185.
7. **Brandenburger, A., D. Legendre, B. Avalosse, and J. Rommelaere.** 1990. NS-1 and NS-2 proteins may act synergistically in the cytopathogenicity of parvovirus MVMp. Virology **174**: 576–584.
8. **Chen, K. C., B. C. Shull, M. Lederman, E. R. Stout, and R. C. Bates.** 1988. Analysis of the termini of the DNA of bovine parvovirus: demonstration of sequence inversion at the left terminus and its implication for the replication model. J. Virol. **62**:3807–3813.
9. **Chen, K. C., J. J. Tyson, M. Lederman, E. R. Stout, and R. C. Bates.** 1989. A kinetic hairpin transfer model for parvoviral DNA replication. J. Mol. Biol. **208**:283–296.
10. **Cotmore, S. F., M. Gunther, and P. Tattersall.** 1989. Evidence for a ligation step in the DNA replication of the autonomous parvovirus minute virus of mice. J. Virol. **63**:1002–1006.
11. **Cotmore, S. F., J. Nüesch, and P. Tattersall.** Unpublished data.
12. **Cotmore, S. F., and P. Tattersall.** 1986. Organization of the nonstructural genes of the autonomous parvovirus minute virus of mice. J. Virol. **58**:724–732.
13. **Cotmore, S. F., and P. Tattersall.** 1987. The autonomously replicating parvoviruses of vertebrates. Adv. Virus Res. **33**:91–174.
14. **Cotmore, S. F., and P. Tattersall.** 1988. The NS-1 polypeptide of minute virus of mice is covalently attached to the 5′ termini of duplex replicative-form DNA and progeny single strands. J. Virol. **62**:851–860.
15. **Cotmore, S. F., and P. Tattersall.** 1989. A genome-linked copy of the NS-1 polypeptide is located on the outside of infectious parvovirus particles. J. Virol. **63**:3902–3911.
16. **DeLange, A. M., M. Reddy, D. Scraba, C. Upton, and G. McFadden.** 1986. Replication and resolution of cloned poxvirus telomeres in vivo generates linear minichromosomes with intact viral hairpin termini. J. Virol. **59**:249–259.
17. **Dickie, P., R. Morgan, and G. McFadden.** 1987. Cruciform extrusion in plasmids bearing the replicative intermediate configuration of a poxvirus telomere. J. Mol. Biol. **196**:541–558.
18. **Diffoot, N., B. C. Shull, K. C. Chen, E. R. Stout, M. Lederman,**

and R. C. Bates. 1989. Identical ends are not required for the equal encapsidation of plus- and minus-strand parvovirus LuIII DNA. J. Virol. **63**:3180–3184.
19. **Eisenberg, S., J. Griffith, and A. Kornberg.** 1977. φX174 cistron A protein is a multifunctional enzyme in DNA replication. Proc. Natl. Acad. Sci. USA **74**:3198–3202.
20. **Eisenberg, S., and A. Kornberg.** 1979. Purification and characterization of φX174 gene A protein. A multifunctional enzyme of duplex DNA replication. J. Biol. Chem. **254**:5328–5332.
21. **Faust, E. A., and D. C. Ward.** 1979. Incomplete genomes of the parvovirus minute virus of mice: selective conservation of genome termini. J. Virol. **32**:276–292.
22. **Felgner, P. L., and M. Holm.** 1989. Cationic liposome-mediated transfection. Focus **11**:21–27.
23. **Hermonat, P. L., M. A. Labow, R. Wright, K. I. Berns, and N. Muzyczka.** 1984. Genetics of adeno-associated virus: isolation and preliminary characterization of adeno-associated virus type 2 mutants. J. Virol. **51**:329–339.
24. **Hirt, B.** 1967. Selective extraction of polyoma DNA from infected cell cultures. J. Mol. Biol. **26**:363–369.
25. **Im, D. S., and N. Muzyczka.** 1990. The AAV origin binding protein Rep68 is an ATP-dependent site-specific endonuclease with DNA helicase activity. Cell **61**:447–457.
26. **Labow, M. A., L. H. Graf, and K. I. Berns.** 1987. Adeno-associated virus gene expression inhibits cellular transformation by heterologous genes. Mol. Cell. Biol. **7**:1320–1325.
27. **Labow, M. A., P. L. Hermonat, and K. I. Berns.** 1986. Positive and negative autoregulation of the adeno-associated virus type 2 genome. J. Virol. **60**:251–258.
28. **Maniatis, T., E. F. Fritsch, and J. Sambrook.** 1982. Molecular cloning: a laboratory manual. Cold Spring Harbor Laboratory, Cold Spring Harbor, N.Y.
29. **McFadden, G., D. Stuart, C. Upton, P. Dickie, and A. R. Morgan.** 1988. Replication and resolution of poxvirus telomeres. Cancer Cells **6**:77–85.
30. **Merchlinsky, M., C. F. Garon, and B. Moss.** 1988. Molecular cloning and sequence of the concatemer junction from vaccinia virus replicative DNA. Viral nuclease cleavage sites in cruciform structures. J. Mol. Biol. **199**:399–413.
31. **Merchlinsky, M., and B. Moss.** 1986. Resolution of linear minichromosomes with hairpin ends from circular plasmids containing vaccinia virus concatemer junctions. Cell **45**:879–884.
32. **Merchlinsky, M., and B. Moss.** 1989. Resolution of vaccinia virus DNA concatemer junctions requires late-gene expression. J. Virol. **63**:1595–1603.
33. **Merchlinsky, M., and B. Moss.** 1989. Nucleotide sequence required for resolution of the concatemer junction of vaccinia virus DNA. J. Virol. **63**:4354–4361.
34. **Rhode, S. L., III.** 1985. *trans*-Activation of parvovirus P_{38} promoter by the 76K noncapsid protein. J. Virol. **55**:886–889.
35. **Rhode, S. L., III.** 1989. Both excision and replication of cloned autonomous parvovirus DNA require the NS1 (Rep) protein. J. Virol. **63**:4249–4256.
36. **Samulski, R. J., L. S. Chang, and T. Shenk.** 1989. Helper-free stocks of recombinant adeno-associated viruses: normal integration does not require viral gene expression. J. Virol. **63**:3822–3828.
37. **Shade, R. O., M. C. Blundell, S. F. Cotmore, P. Tattersall, and C. R. Astell.** 1986. Nucleotide sequence and genome organization of human parvovirus B19 isolated from a child with aplastic crisis. J. Virol. **58**:921–936.
38. **Siegl, G., R. C. Bates, K. I. Berns, B. J. Carter, D. C. Kelly, E. Kurstak, and P. Tattersall.** 1985. Characteristics and taxonomy of Parvoviridae. Intervirology **23**:61–73.
39. **Snyder, R. O., D. S. Im, and N. Muzyczka.** 1990. Evidence for covalent attachment of the adeno-associated virus (AAV) Rep protein to the ends of the AAV genome. J. Virol. **64**:6204–6213.
40. **Snyder, R. O., R. J. Samulski, and N. Muzyczka.** 1990. In vitro resolution of covalently joined AAV chromosome ends. Cell **60**:105–113.
41. **Stow, N. D., M. D. Murray, and E. C. Stow.** 1986. Cis-acting signals involved in the replication and packaging of herpes simplex virus type-1 DNA, p. 497–507. *In* M. Botchan, T. Grodzicker, and P. A. Sharp (ed.), DNA tumor viruses: control of gene expression and replication. Cold Spring Harbor Laboratory, Cold Spring Harbor, N.Y.
42. **Straus, S. E., E. Sebring, and J. Rose.** 1976. Concatamers of alternating plus and minus strands are intermediates in adenovirus-associated virus DNA synthesis. Proc. Natl. Acad. Sci. USA **73**:742–746.
43. **Tattersall, P., and J. Bratton.** 1983. Reciprocal productive and restrictive virus-cell interactions of immunosuppressive and prototype strains of minute virus of mice. J. Virol. **46**:944–955.
44. **Tattersall, P., and D. C. Ward.** 1976. Rolling hairpin model for replication of parvovirus and linear chromosomal DNA. Nature (London) **263**:106–109.
45. **Tratschin, J. D., I. L. Miller, and B. J. Carter.** 1984. Genetic analysis of adeno-associated virus: properties of deletion mutants constructed in vitro and evidence for an adeno-associated virus replication function. J. Virol. **51**:611–619.
46. **Tratschin, J. D., J. Tal, and B. J. Carter.** 1986. Negative and positive regulation in *trans* of gene expression from adeno-associated virus vectors in mammalian cells by a viral rep gene product. Mol. Cell. Biol. **6**:2884–2894.
47. **Tyson, J. J., K. C. Chen, M. Lederman, and R. C. Bates.** 1990. Analysis of the kinetic hairpin transfer model for parvoviral DNA replication. J. Theor. Biol. **144**:155–169.
48. **Ward, D. C., and D. Dadachanji.** 1978. Replication of minute virus of mice DNA, p. 297–313. *In* D. C. Ward and P. Tattersall (ed.), Replication of mammalian parvoviruses. Cold Spring Harbor Laboratory, Cold Spring Harbor, N.Y.
49. **Wigler, M., A. Pellicer, S. Silverstein, R. Axel, G. Urlaub, and L. Chasin.** 1979. DNA-mediated transfer of the adenine phosphoribosyltransferase locus into mammalian cells. Proc. Natl. Acad. Sci. USA **76**:1373–1376.